Journal of ELECTRONIC MATERIALS, Vol. 45, No. 1, 2016
DOI: 10.1007/s11664-015-4199-1

Study on the Conductance and Photo-Conductance of ZnO Thin Films at Different Temperatures in Air and N_2-Atmosphere

S.E. BURRUEL-IBARRA,[1] C. CRUZ-VÁZQUEZ,[1,4] R. BERNAL,[2] R. ACEVES,[2] V.R. ORANTE-BARRÓN,[1] H. GRIJALVA-MONTEVERDE,[1] T.M. PITERS,[2,5] and V.M. CASTAÑO[3,6,7]

1.—Departamento de Investigación en Polímeros y Materiales, Universidad de Sonora, Apartado Postal 130, 83000 Hermosillo, Sonora, Mexico. 2.—Departamento de Investigación en Física, Universidad de Sonora, Apartado Postal 5-088, 83190 Hermosillo, Sonora, Mexico. 3.—Departamento de Física Aplicada y Tecnología Avanzada, Instituto de Física de la Universidad Nacional Autónoma de México, Apartado Postal 1-1010, 76000 Querétaro, Querétaro, Mexico. 4.—e-mail: cathy@correom.uson.mx. 5.—e-mail: piters@cajeme.cifus.uson.mx. 6.—e-mail: castano@fata.unam.mx. 7.—e-mail: meneses@servidor.unam.mx

We report the photoconductance of ZnO thin films obtained from thermally treated ZnS films grown by a chemical bath deposition method. The measurements of photo-conductance were performed in an atmosphere of air or nitrogen (N_2) at different temperatures between 300 K and 375 K. The augmented conductance after ultraviolet (UV) irradiation (330–380 nm) in air fades away slowly to its original value, whereas in a nitrogen atmosphere, a significant part of the augmented conductance remains. Measurements of electrical conductance as a function of temperature in N_2 or air, in the dark or the light, seem to indicate that the donor concentration is increased during the UV irradiation, suggesting that oxygen vacancies and interstitials are created. An alternative model for the photoconduction in ZnO is proposed in which the slow increase of conduction during irradiation is explained by an increase of donors instead of photoelectrons. In this model, the photoelectrons would only play a role in the mechanism of the creation of donors.

Key words: ZnO, conductance, photoconductance

INTRODUCTION

ZnO has received much attention due to its potential application in electronic devices such as lasers and diodes operating in the ultraviolet (UV) and blue regions of the spectrum, transparent conductive electrodes, surface electro-acoustic wave devices, gas sensors, solar cells and piezoelectric transducers.[1–3] One of the interesting features of thin films of this material (and other oxides) is the slow photo-response. This slow response has been attributed to the involvement of oxygen at the surface of the film.[4] Most models that explain the slow photo-response assume the presence of oxygen vacancies and Zn interstitials acting as donors.[4] However, the donated electrons are bound to adsorbed oxygen at the surface forming chemically bound O_2^-. Near the surface, a depletion region is thus formed that could extend over the whole width of the film resulting in a low conductivity. During the irradiation, electrons and holes are created of which the holes recombine with the bounded electrons. During this process, the chemical bound of the oxygen with the surface (chemisorption) is thus removed; however, the oxygen may remain physically bound (physisorption). The photo-generated electrons remain in the bulk and cause the increase of conductance. After irradiation, the physisorbed oxygen molecules may again trap an electron to again get chemically bound, resulting in a decrease of conductance.[4–7] This model has been mainly based on photo-conductance measurements in different gaseous environments and can explain most

(Received June 9, 2015; accepted October 29, 2015; published online November 19, 2015)

of the observed effects. However, only a few investigations include temperature effects.

Since the adsorption and desorption processes are expected to be thermally activated, a study into the effect of temperature on the conductance could gain, or reinforce, insight into the mechanism of the slow response photo-conductance of ZnO. With this objective in mind, we performed the present study in which we investigated the behavior of the photo-conductance during cooling and heating in the temperature range from 300 K to 375 K.

SAMPLE PREPARATION AND STRUCTURAL ANALYSES

To obtain the ZnO films used in this investigation, first, ZnS films were grown on a glass substrate by the chemical bath deposition (CBD) method.[8] To convert the ZnS films to ZnO, the films were thermally treated in air at 400°C for 6 h. The x-ray diffraction (XRD) patterns were collected with a Rigaku Geigerflex diffractometer equipped with a graphite monochromator by using CuKα radiation (λ = 1.542 Å). Scanning electron microscope (SEM) images and the samples compositions were obtained using a JEOL JSM-5410LV scanning electron microscope equipped with an Oxford energy dispersive spectroscopy (EDS) analyzer operating at 15 keV.

Figure 1 shows SEM images of the surface of a film before and after the thermal treatment. It is seen that the thermal treatment does not change the granular and porous structure of the film surface very much; however, cracks appear on a μm scale due to the reduction of the volume during the ZnS to ZnO conversion.

Figure 2 shows the XRD pattern of a ZnO film fabricated with the above-described method together with the diffraction pattern of the ZnS film before the thermal treatment and the reference lines of ZnO (JCPDS # 36-1451) and ZnS. It is seen from this figure that, during the thermal treatment, crystalline ZnO is formed while the original ZnS film has a slightly amorphous structure. According to our EDS analyses, only a molar fraction of 35% of the ZnS on the film converts to ZnO during the thermal treatment. Thus, our films may be thought of as being composed of slightly amorphous ZnS grains covered with a layer of crystalline ZnO.

CONDUCTANCE MEASUREMENTS

For the conductance and photo-conductance measurements, gold electrodes were evaporated on the ZnO film on which thin copper wires were pasted with silver paint. For the photo-conductance measurements, the substrate was mounted on a heater. This heater was located in a box in which the environment could be controlled by flows of nitrogen or air. For illumination of the sample, we used a Xenon lamp operating at 300 W and monochromated with a 03FCG001-type band filter with a transmission range of 330–380 nm. The conductance was determined by the voltage drop over a known resistor (330 kΩ) in series with the sample. The voltage over the sample was in the range from 10.5 V to 12 V.

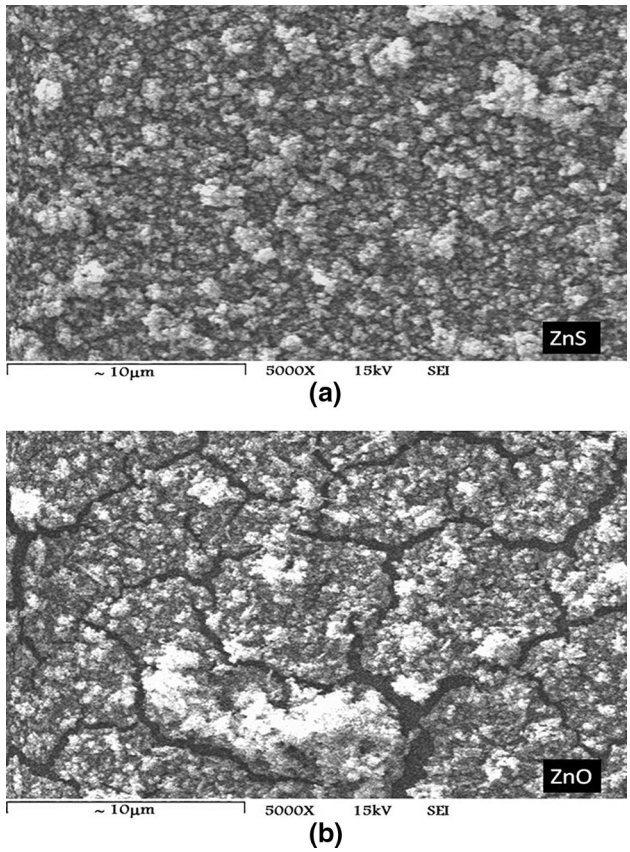

Fig. 1. Scanning electron microscopy images of ZnS film, as obtained before the thermal treatment (a), and the ZnO film obtained after the thermal treatment of the ZnS film (b).

Figure 3 shows the electrical conductance measurements of the ZnO film in air during heating and cooling. These measurements were performed during heating and cooling at rates of 0.1 K/s and 0.02 K/s. It is seen from the figure that the conductance strongly depends on the temperature but only slightly on the path to which the temperature is reached. Furthermore, the conductance behaves more or less according to Boltzmann statistics (data points are on a straight line using the scales of Fig. 3), indicating the presence of donors in the ZnO layer. (The ZnS films before the thermal treatment did not show any conductance, so the measured conductance comes from the ZnO layer.) The three most prominent donors in the ZnO layer are the chemisorbed O_2^- molecule, the oxygen vacancy V_{Ox} and the Zn interstitial I_{Zn}. Fitting the electrical conductance curves of Fig. 1 to $G = G_0 \cdot \exp(-E/kT)$ gives a value for the energy of 0.29 eV. To estimate the activation energy of the related donor, one has to realize that the conductance is the product of the electron concentration and the mobility. If we take

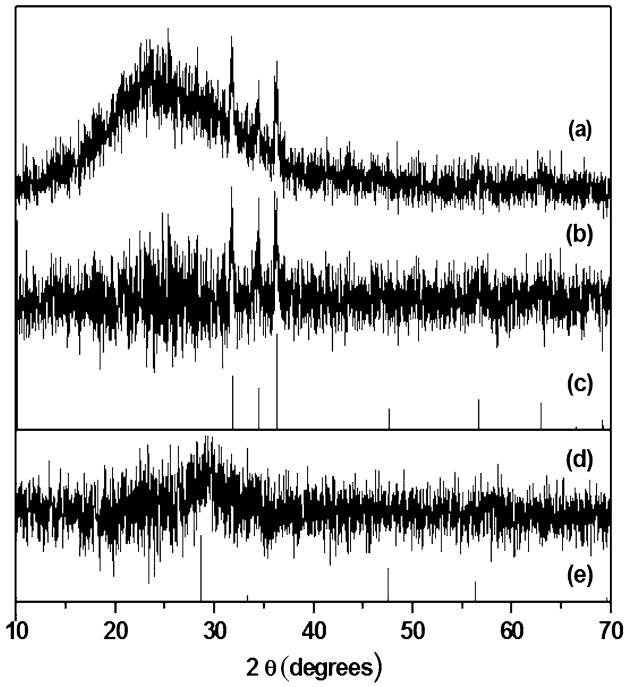

Fig. 2. X-ray diffraction patterns of (a) ZnO film on glass substrate, (b) ZnO film with the background of the substrate subtracted, (c) zincite reference, (d) ZnS film before thermal treatment, (e) ZnS reference.

for the mobility the bulk mobility in pure ZnO, then electron concentration would be determined by $G{\cdot}\mu_0 \exp(\alpha/kT)$ with α approximately 0.072 eV (determined from the figure in Look et al. 1998).[9] For a thin ZnO layer, a similar value for α could be determined.[10] Correcting for this, we find, for the activation energy of the corresponding donor, 0.36 eV which corresponds to the activation energy of the oxygen vacancy donor.[11] Performing the same measurements in an N_2 atmosphere leads to a similar behavior at high temperature (>353 K), and a slow increase of the electrical conductance is observed. This is probably due to the removal of oxygen at the surface.

Figure 4 shows the conductance measurements of the ZnO film in a nitrogen atmosphere after annealing it for different periods at 373 K to remove the oxygen. From this figure, it is seen that, after two annealing periods of 800 s, the conductance increases by about 3 times. In view of the established model, this suggests that the O_2^- electron source concentration would have been reduced significantly during this period. In contrast, the growing rate of the conductance with temperature (dG/dT) increased during this period (also by about 3 times, which is reflected in a constant shift of the data to higher conductance over the whole temperature range when using the scales of Fig. 2). Since one expects that dG/dT is proportional to the donor concentration, we may conclude that the chemisorbed oxygen O_2^- does not contribute much as a

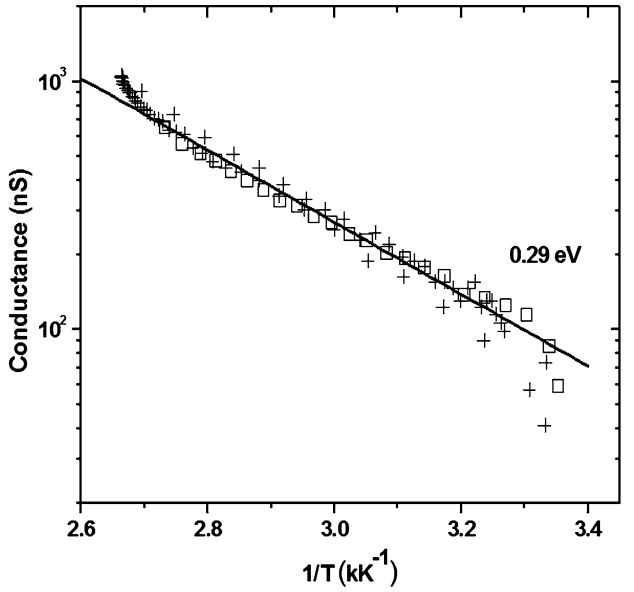

Fig. 3. Conductance of the ZnO film in air during heating and cooling at heating and cooling rates of 0.02 K/s (□) and 0.1 K/s (+).

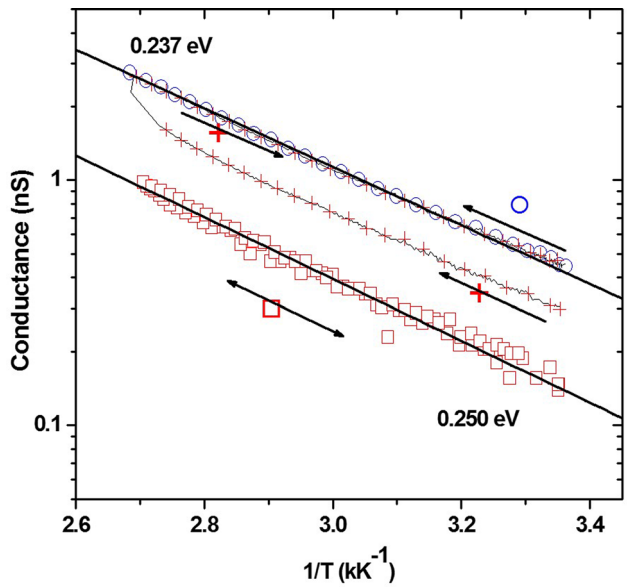

Fig. 4. Conductance of the ZnO film in N_2 atmosphere after: flushing it 300 s with N_2 at RT (□, during heating and cooling), 800 s annealing at 373 K (100°C) (+, during heating) and an additional annealing for 800 s (+, during cooling and ○ during heating). All cooling and heating rates are 0.03 K/s.

donor to the conductance of the film. The energy deduced from the slopes of the curves in Fig. 4 is 0.250 eV after moderate reduction and 0.237 eV after stronger reduction, corresponding to effective activation energy of 0.322 eV and 0.309 eV, respectively. This is lower than the activation energy found in air, suggesting that at least two types of donors are involved. Possibly, there is a contribution of the single ionized Zn interstitial that has an activation energy of 0.22 eV.[11]

To investigate the origin of the radiation-induced persistent conductance of the ZnO film, we measured the conductance during heating and cooling after UV irradiation. Figure 5 shows the change of electrical conductance during the heating and cooling cycle of two measurements with different heating and cooling rates. The measurement containing segments a and b was performed with maximal heating and cooling rates to prevent as much as possible decay of the conductance during the measurement. At the beginning of the heating (segment a), we see an initial increase of the conductance probably caused by the release of electrons from donors. This suggests that, during the UV irradiation, the concentration of donors has grown by photo-generation of V_{Ox} or I_{Zn} defects. After about 340 K, the electrical conductance starts to decrease, indicating either an increase of the annihilation rate of the donors with their counter parts (for the oxygen vacancy donor, V_{Ox} this would be the oxygen interstitial I_{Ox}) or the decrease of available electrons due to the recombination with holes. This is interpreted as the increasing of the release rate at higher temperature of either the trapped counterpart of the donor or the trapped hole. Although the annihilation also continues during cooling (segment b), a reasonable exponential decay with respect to 1/T is observed. The corresponding energy is about 0.25 eV, which suggests that the donors generated during the reduction in the N_2 atmosphere are of the same type as the photo-generated donors. The second measurement (segments d, e and f) was measured with a heating and cooling rate of 0.01 K/s. This was so slow that, during the heating (segment d), the annihilation process of the photo-generated donors dominated over the thermal activated electron release.

Figure 6 compares three measurements of the isothermal decrease of conductance. One was performed in an N_2 atmosphere after a UV irradiation pulse, one in air after a UV irradiation pulse and one in air after reduction in an N_2 atmosphere. All data displayed in Fig. 6 were collected at 368 K (95°C). It can be seen from the figure that the conductance data contain a fast decay component, a slow decay component and an asymptote to which the signal levels off. Fitting while sharing the decay time constants between measurements and assuming first order processes (exponential decay) results in good fitting curves (see Fig. 6), with time decay constants of 187 ± 2 s for the fast decay and 2078 ± 12 s for the slow decay. The values of the asymptotes of the measurements in air are 1.45 (b) and 1.46 nS (c) which are somewhat higher than the dark conductance of 1.0 nS at 368 K (95°C). This indicates that the presumed asymptote in reality represents a very slow decay.

The conductance measurements after the reduction (Fig. 6c) only presented a very small contribution of the fast decay. This may be due to the reduction being a very slow process so that the donor traps participating in the fast decay have already been annihilated before the measurement started. Further, it is seen that, in an N_2 atmosphere, the conductance after the light pulse is much higher than in air. Nevertheless, the initial decrease of conductance is 1.54 times greater than in air. This last observation is contrary to the idea that the decrease in conductance is the result of physisorbed oxygen trapping electrons, since one would expect a lower concentration of surface oxygen in an N_2 atmosphere than in air. Instead, it is suggested that the annihilation of the donor with its counterpart is responsible for the decay of the conductance. It is remarkable that the slow decay component is present in the conductance decay measurements after reduction as well as after photo-stimulation in air and in nitrogen atmosphere. If we assume that this decay component has the same origin in all measurements, then it is clear that it is not directly caused by the return of oxygen from the environment (because it is present in the N_2 environment), although it is stimulated by its presence (because it is present in air after the reduction).

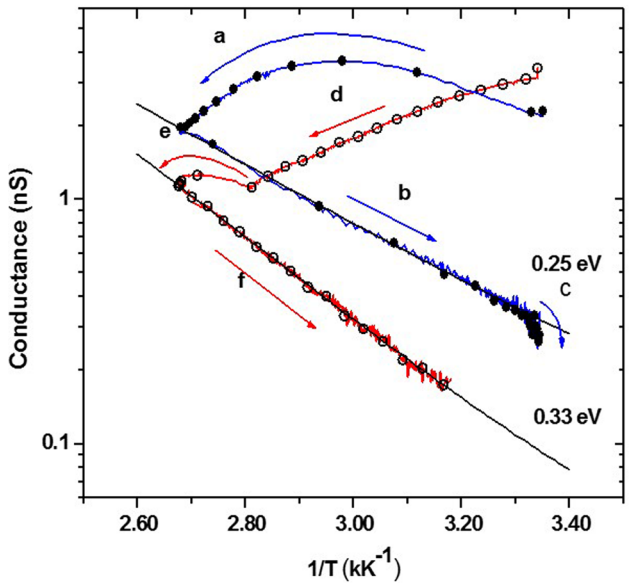

Fig. 5. Electrical conductance during the heating and the cooling of an irradiated ZnO thin film. Segments a, b and c belong to the cycle with the greatest heating and cooling rates and segments d, e and f belong to a cycle with a heating and cooling rate of 0.01 K/s. During segment e, the film was heated quickly from 348 K to 373 K. The ines fitting the cooling stages (segments b and f) correspond to a thermally stimulated process of releasing electrons with the indicated activation energies. Segment c represents isothermal decay. The data points are 400 s apart.

ANALYSIS OF DATA AND DISCUSSION

Our results suggest that the measured photo-induced increment of conductance reflects the increment of donors and not the increment of photoelectrons as assumed in most models of

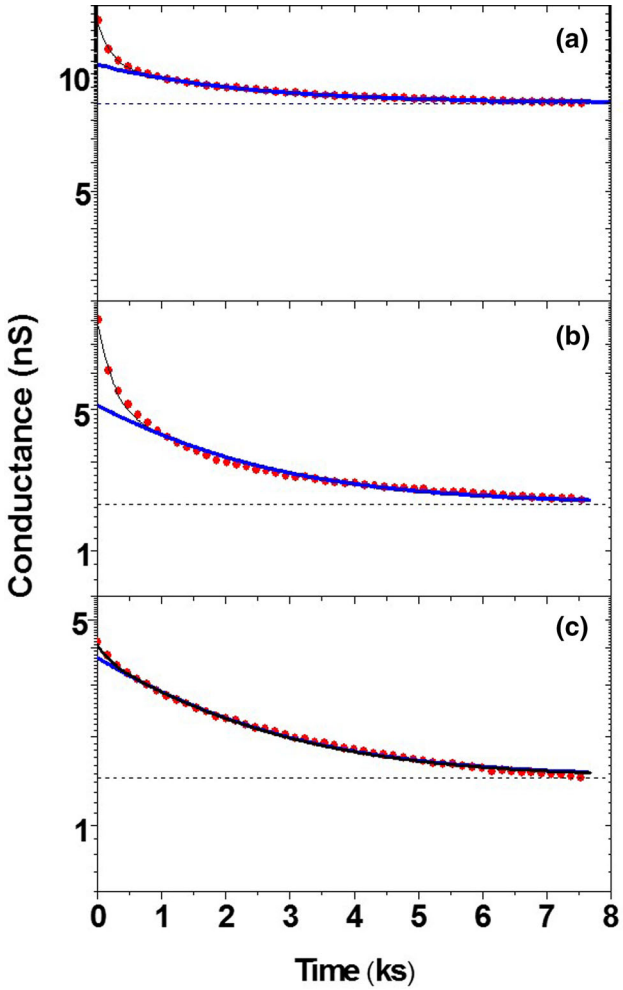

Fig. 6. Measurements of isothermal decay of conductance. (a) In N_2 atmosphere after UV irradiation for 1 s, (b) the same as (a) but in air, and (c) in air after reduction in N_2 atmosphere for 72 ks (20 h) at 368 K. The temperature during all measurements was 368 K (95°C). Dots are measurements, solid lines are fitted curves using two exponential decays and an asymptote, dashed lines are components of the fitted curves, i.e. the asymptote and the asymptote plus the slowest decay.

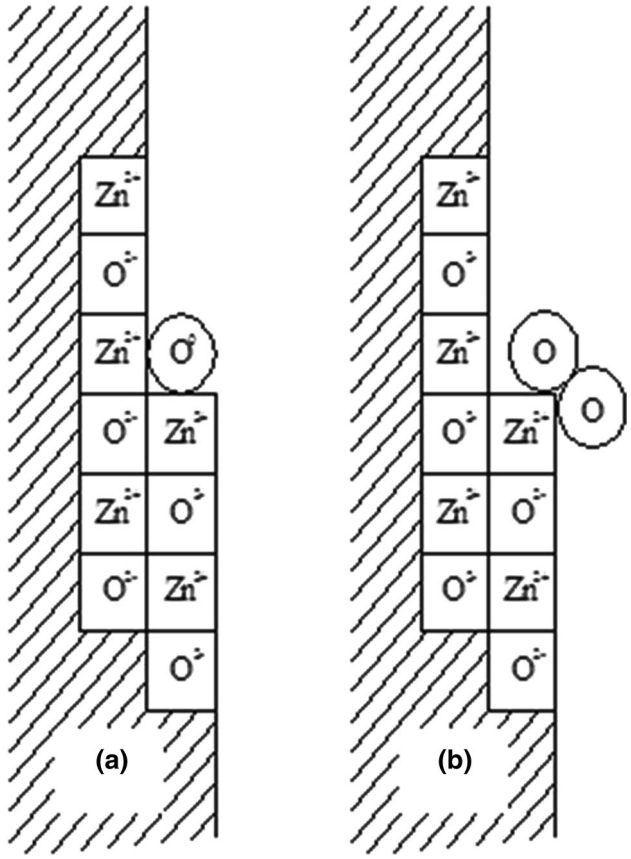

Fig. 7. Oxygen trap at the ZnO surface. (a) Interstitial from the bulk trapped at the surface. (b) Physisorbed oxygen molecule from the atmosphere.

photoconductivity in ZnO. Furthermore, our results suggest that it is the annihilation of the donor with its counterpart that causes the decay of conductance and not the release of holes from (physisorbed) oxygen at the surface. These observations lead to the hypothesis that donors and their counterparts are created during the photo-excitation. To explore this idea, we will assume for simplicity that the created donor–counterpart pair (with the 0.36-eV donor) is a V_{Ox}–I_{Ox} pair and that this pair can be created during UV irradiation by an excitonic mechanism similar to that of the radiation-induced F and H center creation in ionic crystals.[12,13] If we assume that the I_{Ox} is mobile, then it can recombine with a V_{Ox} or migrate to the surface where it may be trapped. If the concentration of I_{Ox} at the surface is sufficiently high, O_2 gas may be formed that could escape from the surface. The arisen surplus of V_{Ox} donors in the bulk near the surface then causes the increase of the conductance. The trapping of I_{Ox} at the surface is much more effective in an atmosphere with a low concentration of oxygen, i.e. on a surface with few adsorbed oxygen. This could be understood if we assume that the physisorbed oxygen from the atmosphere occupies the same site as the trapped interstitial J_{Ox}. Such a site could, for example, be a step in the surface, sided by Zn ions as schematically shown in Fig. 7a. Another such a side is suggested by calculations of Yan et al. They found that the V_{Ox} at the surface acts as an effective trapping site for O_2 molecules (see Fig. 7b).[14] Obviously, such a site would also be a good trap for I_{Ox}.

The formation of V_{Ox}–I_{Ox} pairs during the reduction in the dark would be a pure thermal process. At first sight, this may seem unlikely, since the concentration of V_{Ox} in the bulk is expected to be frozen below 500 K because of the corresponding high formation energy.[15] However, theoretical calculations show that the V_{Ox} formation energy at the surface is about half that in the bulk.[14] So it would not be unreasonable to assume that *near* the surface the activation energy for the formation of V_{Ox}–I_{Ox} pairs would be sufficiently low to actually form V_{Ox}–

I_{Ox} pairs spontaneously at the temperature of the experiment (370 K).

If this formation process is in equilibrium with the annihilation process, and the I_{Ox} trapping process at the surface is in equilibrium with the releasing process, then increasing the concentration of available surface traps (by reduction) results in a shift of the equilibrium in favor of the V_{Ox} concentration. The decay of the conductance shown in Fig. 6 was tentatively described by three independent first-order processes. In view of the above-suggested model, these processes would be the V_{Ox}–I_{Ox} recombination in the bulk (fast), the releasing of I_{Ox} at the surface (slow), and the conversion of adsorbed oxygen molecules to the bulk oxygen atoms (very slow). Strictly speaking, these three processes are not independent and may be treated as such only if the time scales at which they occur are very different. The processes are also not expected to be of first-order. A better but still simple description of the decay would be in terms of the following set of differential equations:

$$\begin{aligned}
\frac{dV}{dt} &= k_{cre} - k_{rec} IV \\
\frac{dI}{dt} &= k_{cre} - k_{rec} IV - k_{trp} I(N - J - M) + k_{esc} J \\
\frac{dJ}{dt} &= k_{trp} I(N - J - M) - k_{esc} J - k_{ass} J^2 + 2k_{dis} M \\
\frac{dM}{dt} &= k_{ass} J^2 - 2k_{dis} M - k_{des} M + k_{ads}(N - J - M)
\end{aligned} \tag{1}$$

in which I is the concentration of I_{Ox}, V is the concentration of V_{Ox}, J is the concentration of trapped I_{Ox}, N is the concentration of available trapping sites (including the empty and full traps), M is the concentration of physisorbed oxygen at the surface, k_{rec} is the I_{Ox}–V_{Ox} recombination rate constant, k_{trp} is the trapping rate constant for I_{Ox} at empty trapping sites at the surface, k_{esc} is the release rate of trapped I_{Ox} at the surface, k_{cre} is the creation rate of V_{Ox}–I_{Ox} pairs, k_{ass} is the association rate constant for the reaction $2J_{Ox} \rightarrow O_2$ where J_{Ox} is a trapped oxygen interstitial at the surface, k_{dis} is the dissociation rate constant of physisorbed oxygen describing the reaction $O_2 \rightarrow 2J_{Ox}$, k_{des} is the desorption rate constant of physisorbed O_2 and k_{ads} is the adsorption rate constant. This set of differential equations would also describe the rise of conductance during reduction and during irradiation.

The processes involving chemisorbed oxygen playing a crucial role in the cited literature do not appear explicitly in the set of equationsproposed here to describe the conductance. It is here assumed that the chemisorbed oxygen is so tightly bound that it remains stable up to the highest temperature of 375 K used in this investigation. To analyze the data of Fig. 6, we solved the differential Eq. 1 numerically, using the Bulirsch-Stoer method, with a backward (implicit) Euler scheme for the integration step,[16] and fitted the parameter values so that the calculated V_{Ox} concentrations fitted to all data of Fig. 4 simultaneously.

Figure 8 show the fitting result of the differential Eq. 1 to the measurements of Fig. 6. Figure 8a shows the concentrations of V_{Ox}, I_{Ox} and J_{Ox} after an irradiation pulse in N_2 atmosphere, Fig. 8b shows the concentrations after an irradiation pulse in air, and Fig. 8c shows the concentrations after changing the sample from a N_2 atmosphere to air. The fitting parameters are: $k_{cre} = 9.38 \times 10^{-2}\ \mu s^{-1}$, $k_{rec} = 2.53 \times 10^{-3}\ \mu^{-1}\ s^{-1}$, $k_{trp} = 2.53 \times 10^{-3}\ \mu^{-1}\ s^{-1}$, $k_{esc} = 4.68 \times 10^{-3}\ s^{-1}$, $N = 410\ \mu$, $k_{ass} = 2.35 \times 10^{-5}\ \mu^{-1}\ s^{-1}$, $k_{dis} = 5.17 \times 10^{-4}\ s^{-1}$, $k_{des} = 9.40 \times 10^{-4}\ s^{-1}$, $k_{ads1} = 1.79 \times 10^{-4}\ \mu s^{-1}$, $k_{ads2} = 1.2 \times 10^{-3}\ \mu s^{-1}$, $k_{pcr} = 1.67 \times 10^{9}\ \mu s^{-1}$. The unit μ is an arbitrary unit of concentration. The I_{Ox} concentration was less than 1 μ (not shown). Figure 9 show the same as Fig. 8 but with the fitting parameters: $k_{tcr} = 5.45\ \mu s^{-1}$, $k_{rec} = 3.88 \times 10^{-4}\ \mu^{-1}\ s^{-1}$, $k_{trp} = 1.6 \times 10^{-8}\ \mu^{-1}\ s^{-1}$, $k_{esc} = 1.8 \times 10^{-3}\ s^{-1}$, $N = 36310\ \mu$, $k_{ass} = 1.48 \times 10^{-5}\ \mu^{-1}\ s^{-1}$, $k_{dis} = 0.398\ s^{-1}$, $k_{des} = 1.48\ s^{-1}$, $k_{ads1} = 2.11 \times 10^{-6}\ \mu s^{-1}$, $k_{ads2} = 2.06 \times 10^{-5}\ \mu s^{-1}$, $k_{pcr} = 7.31 \times 10^{8}\ \mu s^{-1}$.

The fittings were carried out with the routine FATAL (from "fits anything to anything you like")[17] embedded in our fitting program TAMTAM (from "tests any model to any measurement"). As a boundary condition, we assumed equilibrium at the beginning of the measurement (except for the J_{Ox} concentration of measurement c to allow for some flexibility) from which the concentrations at $t = 0$ were determined. During decay, the parameter k_{cre} was assumed to be the thermal creation rate k_{tcr} of I_{Ox}–V_{Ox} pairs, while during the irradiation pulse, k_{cre} was assumed to be the sum of thermal- plus photo-creation rate k_{pcr} of I_{Ox}–V_{Ox} pairs. The irradiation time was fixed at 0.5 s. Further, the parameter k_{ads} was taken as different for a nitrogen atmosphere (k_{ads1}) than for an oxygen atmosphere (k_{ads2}). So, in total, there are 11 parameters to be fitted: k_{tcr}, k_{pcr}, k_{rek}, k_{trp}, k_{esc}, k_{ass}, k_{des}, k_{ads1}, k_{ads2} and N. Additionally, the fitting gave us the concentrations I_{Ox}, J_{Ox} and M_{Ox}. The fitting converged to two different solutions. This is a consequence of the many chained reactions in the set of differential equations and the restriction of measuring only one reaction product. Apparently, one of the reactions is so fast that it may be considered in equilibrium on the time scales of the experiment. The processes are thus determined by one equation less. In the first solution, the I_{Ox} concentration is in quasi-equilibrium due to the relative high recombination rate. This solution requires a high mobility of the interstitial and could be obtained with a reduced set of differential equations:

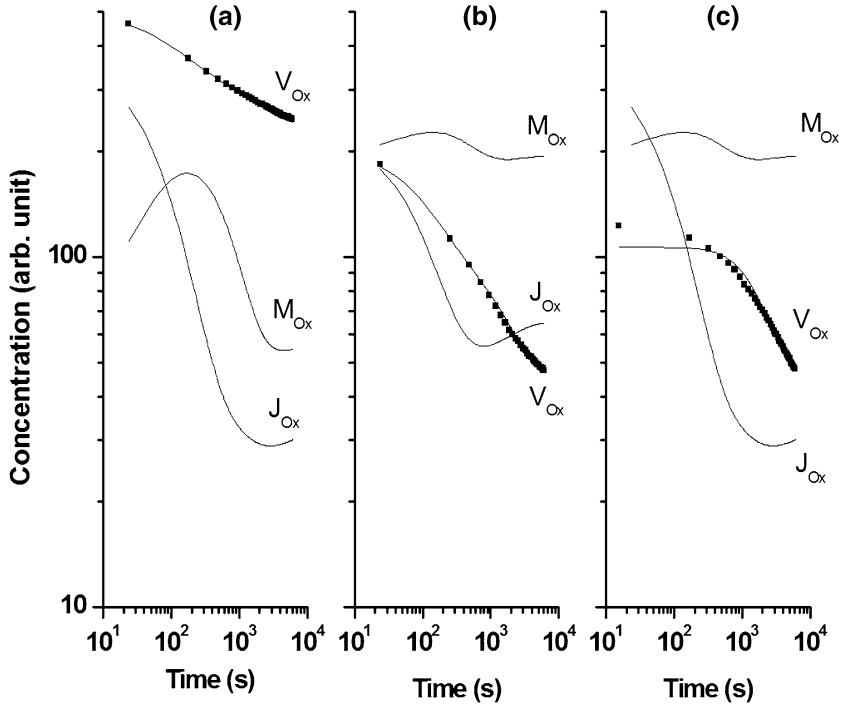

Fig. 8. Fitting result of the differential Eq. 1 to the measurements of Fig. 6. (a) The concentrations of V_{Ox}, I_{Ox} and J_{Ox} after an irradiation pulse in N_2 atmosphere, (b) the concentrations after an irradiation pulse in air and (c) the concentrations after changing the sample from a N_2 atmosphere to air. The fitting parameters are: $k_{cre} = 9.38 \times 10^{-2}\ \mu s^{-1}$, $k_{rec} = 2.53 \times 10^{-3}\ \mu^{-1}\ s^{-1}$, $k_{trp} = 2.53 \times 10^{-3}\ \mu^{-1}\ s^{-1}$, $k_{esc} = 4.68 \times 10^{-3}\ s^{-1}$, $N = 410\ \mu$, $k_{ass} = 2.35 \times 10^{-5}\ \mu^{-1}\ s^{-1}$, $k_{dis} = 5.17 \times 10^{-4}\ s^{-1}$, $k_{des} = 9.40 \times 10^{-4}\ s^{-1}$, $k_{ads1} = 1.79 \times 10^{-4}\ \mu s^{-1}$, $k_{ads2} = 1.2 \times 10^{-3}\ \mu s^{-1}$, $k_{pcr} = 1.67 \times 10^{9}\ \mu s^{-1}$. The unit μ is an arbitrary unit of concentration. The I_{Ox} concentration was less than 1 μ (not shown).

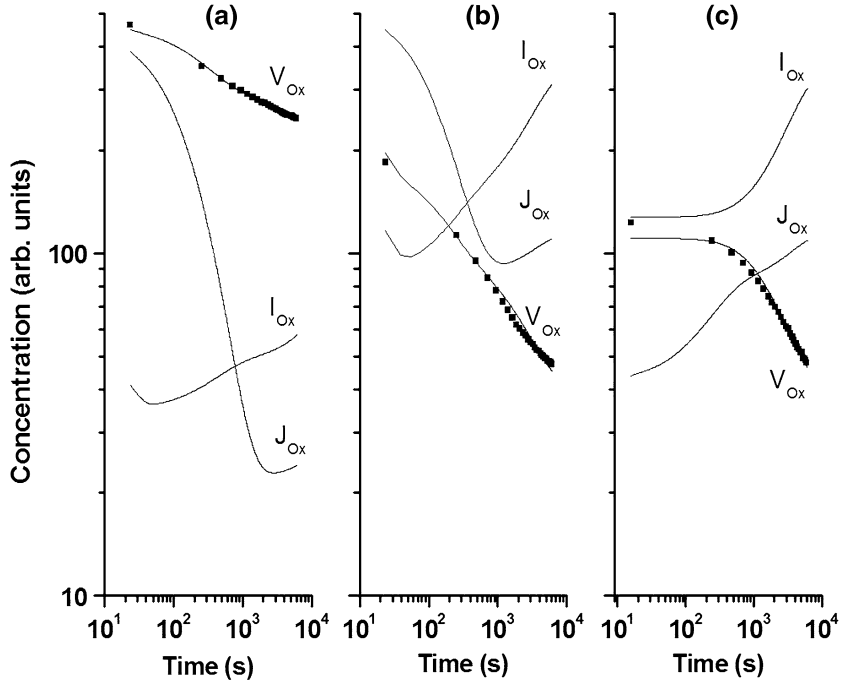

Fig. 9. Fitting result of the differential Eq. 1 to the measurements of Fig. 6. (a) The concentrations of V_{Ox}, I_{Ox} and J_{Ox} after an irradiation pulse in N_2 atmosphere, (b) the concentrations after an irradiation pulse in air and (c) the concentrations after changing the sample from a N_2 atmosphere to air. The fitting parameters are: $k_{tcr} = 5.45\ \mu s^{-1}$, $k_{rec} = 3.88 \times 10^{-4}\ \mu^{-1}\ s^{-1}$, $k_{trp} = 1.6 \times 10^{-8}\ \mu^{-1}\ s^{-1}$, $k_{esc} = 1.8 \times 10^{-3}\ s^{-1}$, $N = 36310\ \mu$, $k_{ass} = 1.48 \times 10^{-5}\ \mu^{-1}\ s^{-1}$, $k_{dis} = 0.398\ s^{-1}$, $k_{des} = 1.48\ s^{-1}$, $k_{ads1} = 2.11 \times 10^{-6}\ \mu s^{-1}$, $k_{ads2} = 2.06 \times 10^{-5}\ \mu s^{-1}$, $k_{pcr} = 7.31 \times 10^{8}\ \mu s^{-1}$. The concentration of M_{Ox} was less than 1 μ (not shown).

$$\begin{aligned}\frac{dV}{dt} &= k_{cre} - k_{esc}J \\ \frac{dJ}{dt} &= k_{cre} - k_{esc}J - k_{ass}J^2 + 2k_{dis}M \\ \frac{dM}{dt} &= k_{ass}J^2 - 2k_{dis}M - k_{des}M + k_{ads}(N - J - M)\end{aligned} \quad (2)$$

In the other solution, the physisorbed oxygen is in quasi-equilibrium due to relative high desorption and dissociation constants. This solution could be obtained with the following set of reduced equations:

$$\begin{aligned}\frac{dV}{dt} &= k_{cre} - k_{rec}IV \\ \frac{dI}{dt} &= k_{cre} - k_{rec}IV - k_{trp}I(N - J) + k_{esc}J \\ \frac{dJ}{dt} &= k_{trp}I(N - J) - k_{esc}J - k_{ass}J^2 + 2k_{ads}(N - J)\end{aligned} \quad (3)$$

Based solely on the fitting results, it is difficult to choose between the two models. The first model requires that the I_{Ox} has a relative high mobility and that a significant quantity of physisorbed oxygen exists as an intermediate step between I_{Ox} and free O_2, which determines for an important part the creation and annihilation rates of oxygen vacancies. For the second mechanism, the I_{Ox} concentration is relative high, while the concentration of physisorbed oxygen does not determine the creation or anihilation rates of oxygen vacancies.

CONCLUSIONS

We arrived at two possible descriptions for photoconductivity in ZnO. In both descriptions, V_{Ox}–I_{Ox} pairs are formed during the UV irradiation of which the V_{Ox} acts as a donor and the increase of its concentration increases the conductance. In the first description, the I_{Ox} is relative mobile and could be trapped at trapping sites near the surface. In the dark, I_{Ox} slowly releases from the trapping sites and recombines with V_{Ox}. The trapping of I_{Ox} is in competition with the physisorption of environmental oxygen. In the second description, the I_{Ox} migrates only slowly through the bulk. In the dark, it can recombine with V_{Ox}. When I_{Ox} reaches the surface, it forms O_2 and can escape to the environment. If oxygen is present in the environment, then oxygen can return to the bulk. In both descriptions, chemisorbed oxygen responsible for the neutralization of latent V_{Ox} would not be affected. That means that, in this description, the process of V_{Ox}–I_{Ox} pair formation in which the recombination of photo-generated electrons and holes are involved would dominate over the process of the recombination of photo-generated holes with ionized (chemisorbed) oxygen at the surface. This picture is mainly based on the observation that, during irradiation, the donor concentration increases and on the observation that the initial decay of conductance after irradiation in N_2 gas is in fact greater than in air. This description of photoconductivity could explain the observations that were previously explained qualitatively by the model used in the referenced literature if one replaces electrons by V_{Ox} and holes by I_{Ox} and applies some trivial adaptations.

ACKNOWLEDGEMENT

We acknowledge the technical support of J. C. Avila-Barrera and M. Atondo-Encinas. All figures and most of our analyses were made with the computer program Origin 6.1 from OriginLab Corporation. This work was supported by Project: PICA 05/DCEN01 (Universidad de Sonora).

REFERENCES

1. F.D. Auret, J.M. Nel, M. Hayes, L. Wu, W. Wesch, and E. Wendler, *Superlattice Microstrut* 39, 17 (2006).
2. C.R. Gorla, N.W. Emanetoglu, S. Liang, W.E. Mayo, Y. Lu, M. Wraback, and H. Shen, *J. Appl. Phys.* 85, 2595 (1999).
3. Y. Ma, W.L. Wang, K.J. Liao, and C.Y. Kong, *J. Wide Bandgap Mater.* 10, 113 (2002).
4. P. Sharma, K. Sreenivas, and K.V. Rao, *J. Appl. Phys.* 93, 3963 (2003).
5. S. Kumar, V. Gupta, and K. Sreenivas, *Nanotechnology* 16, 1167 (2005).
6. S.A. Studenikin, N. Golego, and M. Cocivera, *J. Appl. Phys.* 87, 2413 (2000).
7. Q. Wan, Z.T. Song, W.L. Liu, C.L. Lin, and T.H. Wang, *Nanotechnology* 15, 559 (2004).
8. C. Cruz-Vázquez, F. Rocha-Alonzo, S.E. Burruel-Ibarra, M. Barboza-Flores, R. Bernal, and M. Inoue, *Appl. Phys.* 79, 1941 (2004).
9. D.C. Look, D.C. Reynolds, J.R. Sizelove, R.L. Jones, C.W. Litton, G. Cantwell, and W.C. Harsch, *Solid State Commun.* 105, 399 (1998).
10. T. Edahiro, N. Fujimura, and T. Ito, *J. Appl. Phys.* 93, 7673 (2003).
11. C. Pengfei, L. Shengtao, Z. Le, and L. Jianying, *Appl. Phys. Lett.* 93, 012902 (2008).
12. Y. Kayanuma, *Defect Processes Induced by Electronic Excitation in Insolaters*, vol. 2, ed. N. Itoh (Singapore: World Scientific, 1989), p. 12.
13. K.S. Song and R.T. Williams, Self-Trapped Excitons, Chapters 1, 5, 6 (Berlin, Springer, 1996).
14. Y. Yan, M. Al-Jassim, and S.H. Wei, *Phys. Rev. B.* 72, 161307(R) (2002).
15. H. Geistlinger, *J. Appl. Phys.* 80, 1370 (1996).
16. W.H. Press, B.P. Flannery, S.A. Teukolsky, and W.T. Vetterling, *Numerical Recipes*, vol. 15 (Cambridge: Cambridge University press, 1990).
17. L. Salmon and D.V. Booker, Report No. AERE-R 7129, (Harwell Laboratory, Oxfordshire, 1972).